

Transmission suite design for vibro-acoustic characterization of lightweight panels

C. Gonzalez Diaz¹, M. Vivolo¹, B. Pluymers¹, D. Vandepitte¹, W. Desmet¹

¹ K.U.Leuven, Department Mechanical Engineering
Celestijnenlaan 300 B – box 2420, B-3001, Heverlee, Belgium
email: c.gonzalezdiaz@mech.kuleuven.be

Abstract

This paper concerns with the design of an acoustic cavity (transmission suite) for the vibro-acoustic characterization of lightweight panels. This setup has the big advantage of being a small (1150x984x820 mm) which allows the identification of the studied behaviour for both structure- and air- borne excitation, on panels of different size (from A4 to A2) and thickness (up to 5cm). Particular effort is made for selecting an optimum geometric configuration. Taking into account the acoustic eigenfrequencies' occurrences up to the Schroeder frequency and considering the surface averaged sound absorption coefficient (α) this design leads to the smoothest and most uniform distribution of the natural frequencies of the acoustic cavity. The final design results in a non-parallel walled concrete box of moderate dimensions. Specific care is taken for the implementation and building of the test setup. The resulting facility allows the identification of both structure-borne and air-borne acoustic isolation parameters in lightweight panels of different size.

1 Introduction

Over the past years there has been an increase of production of lightweight structures and materials such as honeycomb or sandwich materials. They seem to be highly attractive for many applications, in the civil [1], aerospace [2-6], and automobile industries [7]. For accurate vibro-acoustic characterisation of these lightweight materials (i.e., Insertion Loss, forced dynamic behaviour and more), this paper discusses the design and implementation of a dedicated transmission suite.

With the acoustic Insertion Loss of a structure, the isolation of incident acoustic power can be quantified. It is defined as the loss of radiated power resulting from the insertion of a device in the transmission line, in this case, due to the insertion of a lightweight component.

The most common technique used to identify the vibro-acoustic properties of a specific system makes use of two finite sized reverberation rooms (or one anechoic source room and a reverberant receiving room) in a sound transmission suite [8-10], where for instance the Transmission Loss can be evaluated. An acoustic field is created by one or several loudspeaker in the source room and transmitted to the receiving room via the examined component. Measurements of both the source and the receiving field (Sound Pressure Level, SPL) give information about the transmission abilities of the tested specimen. Other methods of measuring absorption coefficients use a plane wave which is mostly enclosed in a rigid tube as test field "impedance tube" method [11;12]. These methods are restricted to the examination of small, locally reacting materials with a plane or nearly plane surface, and also to normal wave incidence onto the test specimen.

The new design proposed in this work has the advantage of being a small sized room; therefore it is cheap to build and takes less space and allows to measure samples with different thicknesses (up to 5 cm) and sizes (A4 to A2 dimensions).

The structures to be tested could be excited either by an acoustic field produced by loudspeakers placed inside the acoustic room or directly by a point force generated with a shaker.

Some construction considerations have been taken into account; the acoustic cavity have been constructed out of reinforced concrete in order to achieve nearly perfect reflecting surfaces needed to maintain a prolonged reverberation sound field and a high degree of sound isolation due to the large mass of the reinforced concrete walls. Lately, an alternative to the reinforced concrete construction is to use prefabricated acoustic panels; they have the advantage they can be removed and reinstalled at another site, however they will double the construction price and one might have problems with the sealing between the panels. Also, a second alternative to the reinforced concrete is to employ “lightweight traditional building material” (gypsum drywall), this methods has the advantage to be lower in price than prefabricated acoustic panels, however it does not provide as high degree of sound isolation as the other methods. Pursuing rigid walls enclosing the cavity also facilitates the construction of accurate numerical models.

2 Sound in a rectangular room; the method of analysis

The resonance frequencies (eigenfrequencies) of a rectangular room with dimensions L_x , L_y , L_z can be calculated from the following equation:

$$f_{n_x, n_y, n_z} = \frac{c}{2} \sqrt{\left(\frac{n_x}{L_x}\right)^2 + \left(\frac{n_y}{L_y}\right)^2 + \left(\frac{n_z}{L_z}\right)^2} \quad (1)$$

where c is the sound speed (m/s) and integers n_x , n_y , n_z , represent the order of the modes. As pointed out by Bolt [13-16], the spectral response in each point inside a rectangular room is largely determined by its dimensions and shape. He proposes a chart to choose the proportions between the room dimensions that provides a homogeneous distribution of the normal frequencies inside the room. Basically, this chart provides the relative dimensions of a small rectangular room giving the smoothest frequency response. Bolt’s chart has been further updated by other authors [17]. As discussed by Bolt [13-16], the mean square of the deviations (ψ) of the actual distances between subsequent modes from the mean value in a frequency range is a way to quantify the homogeneity of the eigenfrequencies distribution [14]

$$\psi = \frac{\sum_{i=1}^{n-1} \varepsilon_i^2}{(n-1)\delta^2} + 1, \quad (2)$$

where n - represents the number of the eigenfrequency, i - denotes the index of the pair of eigenfrequencies whose distance is considered, δ is the mean distance between successive eigenfrequencies [Hz] and ε_i - is the variation from the mean value (δ). The mean square of the deviations (ψ) shows that the higher its value the bigger the variations of the frequency spacing in the frequency range taken into account. The frequency domain of interest has a considerable effect on this equation (2). In this paper, the modal analysis is performed in the frequency range up to “the Schroeder frequency” f_{sch} . This critical frequency was derived by Schroeder [18;19] and marks the limit between a frequency range where the room resonances are well-separated and each of them can be individually excited and detected, and that with a strong overlap of resonances, which cannot be separated. Basically it is the limit between diffuse and non-diffuse sound field. This frequency is defined by the following equation [18]:

$$f_{sch} = 2000 \sqrt{\frac{T_{60}}{V}} \quad (3)$$

where T_{60} is the reverberation time in seconds and V the volume of the room in cubic meters. This reverberation time, T_{60} was introduced by Sabine [20] and it is defined as the time interval in which the field SPL drops down by 60 dB:

$$T_{60} = \frac{-0.16V}{S \ln(1-\alpha)}, \quad (4)$$

where S is the total surface of the room in square meters, and α is the absorption coefficient. Substituting equation (4) into equation (3) the Schroeder frequency is given by:

$$f_{sch} = 2000 \sqrt{\frac{-0.16}{S \ln(1-\alpha)}}. \quad (5)$$

According to equation (5) the range of frequency which is taken into account in the modal analysis depends on the total area limiting the room (S) and the absorption coefficient at its walls (α). In large rooms ($\sim 300 \text{ m}^3$) the Schroeder frequency is typically below 50 Hz. Above this threshold there is a strong overlap of natural frequencies, and in this case their exact identification results to be pointless. A good knowledge about the eigenfrequency distribution is of great interest in small rooms. It is the case studied in this paper, where a part of the important frequency range lies below the Schroeder frequency. From equation (5), it can be seen that the higher the value of α the lower Schroeder frequency (f_{sch}).

However in order to study correctly the distributions of the eigenfrequencies, another parameter should be added to the analysis. It is Ω [13] defined as follows:

$$\Omega = \frac{\sum_{i=1}^{n-1} (|\varepsilon_i| - \Lambda)^2}{(n-1)\Lambda}, \quad (6)$$

where

$$\Lambda = \sqrt{\psi - 1}. \quad (7)$$

This value (Ω) shows how big is the “gap” between the eigenfrequencies over the specified frequency range. Basically, the higher the value of Ω , the bigger the “gap”.

3 Optimization

Since Bolt [13] many criteria have been suggested to optimise the proportions of the room dimensions in order to have the smoothest frequency response. Among the other, the optimized ratio proposed by Bolt is {1:1.5:2.5}; this ratio gives values of $\psi = 3,28$ ($\alpha = 0,2$) or $\psi = 1,66$ ($\alpha = 0,6$). A later more refined method based on Bolt’s theory is proposed by Blaszak [17], who suggests {1:1.2:1.4} as a ratio which gives lower value of ψ ; 2.30 ($\alpha = 0.1$). Another interesting value is {1:1.26:1.59} as reported in [21;22].

3.1 Ratio

In this subsection the main aim is to find the smoothest and most uniform distribution of the eigenfrequencies of the acoustic room. In other words, the geometry which gives the lower values of ψ and Ω are found in this subsection. As already mentioned, the best ratios found in the literature are {1:1.2:1.4} [17] and {1:1.26:1.59} [17;21;22]. Starting from this values in this subsection more complex solutions are proposed, also including irregularities in the geometry, for which the application of discretized models and computational procedures (such as the finite element (FEM), and boundary element (BEM), methods) are needed. The study is performed using FEM and BEM softwares, respectively, MD Nastran 3rb and LMS.Virtual Lab Rev8b. Patran 2008 r1 is used for the FE pre- and post-processing. In this subsection, the selection of the optimum geometric proportions of the acoustic room is proposed. The examined frequency range is up to the Schroeder frequency and a realistic surface averaged sound absorption coefficient (α) is taken into account. As already pointed out in the previous section, the higher the value of α , the lower Schroeder frequency (f_{sch}).

Two different set of ratios are studied in this subsection; the one proposed by Blaszak [17] and the one by ANSI [21;22], but just the distributions of the eigenvalues of the first one are shown in this subsection, since it has been proved to have smoother distributions of the eigenfrequencies than the ratio proposed by the American National Standard Institute (ANSI) for the dimensions studied in this paper.

The starting shape has all the walls parallel. The next step is to incline little by little the walls in order to increase the uniformity of the distributions of the eigenfrequencies. For the practicability, the angles between the front wall, where the test samples will be placed, one of the lateral wall and the floor are 90 degrees. Figure 1 shows the best distributions of the eigenfrequencies for the ratio proposed by Blaszk [17] with the following dimensions {1.25:1.50:1.75} for two different values of sound absorption coefficient (α). In both plots (Figure 1), there are four distributions of the eigenfrequencies; “Parallel walls; the angles between all the walls are 90 degrees, “No-Parallels 1”: the back wall is tilted 25cm, the top one 20 cm and the lateral one 5 cm, “No-Parallels 2”: the back wall is tilted 10cm, the top one 20 cm and the lateral one 5 cm and “No-Parallels 3”: the back wall is tilted 10cm, the top one 30 cm and the lateral one 5 cm. From the results obtained, the “No-Parallels 2” has been chosen to be the best since it is the shape which provide the best distribution of the eigenfrequencies, lower value of ψ for different values of sound absorption coefficient (α), even though the gap (Ω) is slightly larger than the one found with the parallel walls. However, this shape has been chosen because there is not overlapping at low frequency, in such a way, once the measurements are taken, the acoustics modes will be identified easily due to the fact that at low frequency they are well-separated. The final dimensions could be found in section 4. The dimensions found in this section as the optimums will not match with the ones shown in section 4, but the same ratio is kept, therefore the same distribution is obtained. The shape has been chosen convex in order to be able to model the system as a unique subsystem using Wave Based Method (WBM) [23].

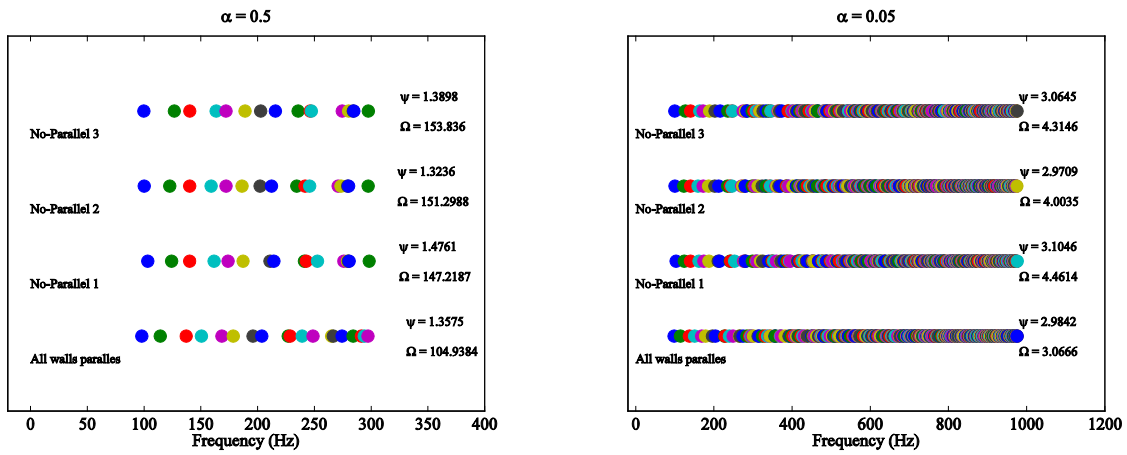


Figure 1: Natural frequency distributions; {1.25:1.5:1.75} Blaszk [17].

3.2 Wall thickness influence

In this subsection the effect of the wall thickness surrounding the room is studied. In order to do that, a model with infinite rigid wall is compared with a model with different wall thicknesses. The test sample used consists of a rectangular aluminium plate with fully clamped boundary conditions. The geometry and the properties of the test sample are summarized in Table 4. As already pointed out the material used for the walls is reinforced concrete and its properties are summarized in the Table 2. In both cases the test samples is excited by an acoustic field provided by an acoustic source located inside the cavity. The displacement is measured by an ideal displacement sensor located on the test sample. The acoustic source's and displacement sensor's locations are kept the same for the consistency of the simulation-measurements.

Figure 2(a,b and c) shows that the thicker the walls, the lower the effects are observed in the frequency response function (FRF) between the displacement sensor located on the test sample and the acoustic

source located inside the cavity. This is due to the fact that increasing the thickness of the walls, also the stiffness of the walls is increased; therefore the system will behave as it had rigid walls. These results were expected, but the main aim of this subsection is to find the optimum thickness of the walls which provides stiff enough cavity walls so that, the sound transmission through the test sample is about 10-20dB (Figure 3) higher than the flanking component radiated by the cavity walls and it does not provide a too heavy setup system, since the increase of the thickness of the cavity walls increases drastically the weight of the acoustic cavity. Table 1 summarises what has been pointed out in this subsection; that the thicker the walls, the better. The second column in Table 1 shows the mean absolute amplitude error at the natural frequencies of the test panel up to 500 Hz between the model with the rigid walls and the model either with 10cm, 12cm or 14cm wall thickness. The second and the third columns show the discrepancy of the natural frequency of the test sample between the rigid walls model and the one with different wall thickness for two different values <1 Hz and <2 Hz, respectively. It is shown, that the thicker the walls, the smaller the variations.

The wall thickness chosen is 15 cm because it supplies well stiff acoustical walls, the final weight is under the values the facilities and instrumentations can support and handle and make more practical the construction of such a test setup.

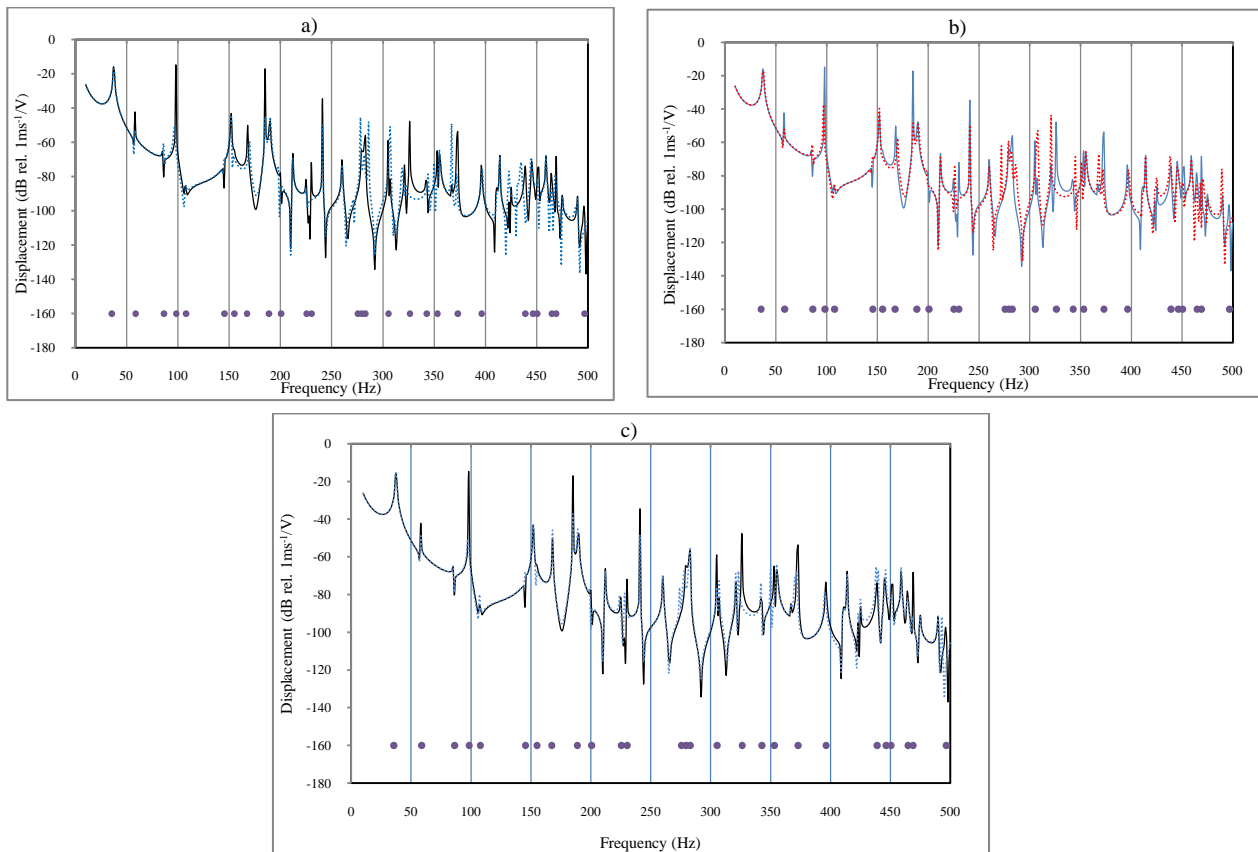


Figure 2: Wall thickness effect; displacement of the test sample clamped to a cavity with rigid walls cavity (solid lines), resonances frequencies of the test sample with clamped boundary conditions (circles), displacement of the test sample clamped to cavity with a) 10 cm thickness, 12 cm thickness and 14 cm thickness.

Thickness walls	Mean abs error (dB) [0-500 Hz]	First 20 modes of the test sample [0-400 Hz]	
		Δ freq.<1Hz	Δ freq.<2Hz
10 cm	5	8 times	12 times
12 cm	5	8 times	12 times
14 cm	3	13 times	14 times

Table 1: Mean absolute amplitude error and natural frequency discrepancy.

3.2.1 Front wall thickness influence; Aluminium us Steel

As was already pointed out in section 1, the set up has a set of 4 front walls made of aluminium (Figure 7, 8, 9 and 10). Each of them has different size windows (A2 to A4 sizes) to accommodated different sizes and thicknesses of test samples. These front walls are made of aluminium mainly because of the practicality point of view. That is, the change from one front wall to other should be done in an easy way, therefore the lighter the better. However, they should supply a very stiff acoustical wall properties in order to fulfil the requirement pointed out in the previous section; the sound transmission through the test sample should be about 10-20dB (Figure 3) higher than the flanking component radiated by the cavity walls. Among the three different materials; reinforced concrete, steel or aluminium, the latter one is chosen. Reinforced concrete is not used as a material due to the fact of the complexity for manufacturing it. Aluminium is lighter than steel (~1/3 lighter) therefore easier to handle it and it fulfils the requirements needed about the stiffness (Figure 3).

Figure 3 shows the forced response measured either on the panel (solid lines) or on the front walls (dashed line). The test sample is excited by point force. The dotted lines, in both plots (a), b)) show the forced response of an ideal test sample with clamped boundary conditions. From these plots it can be seen that the requirement pointed out before is fulfilled for both materials in the frequency range of interest.

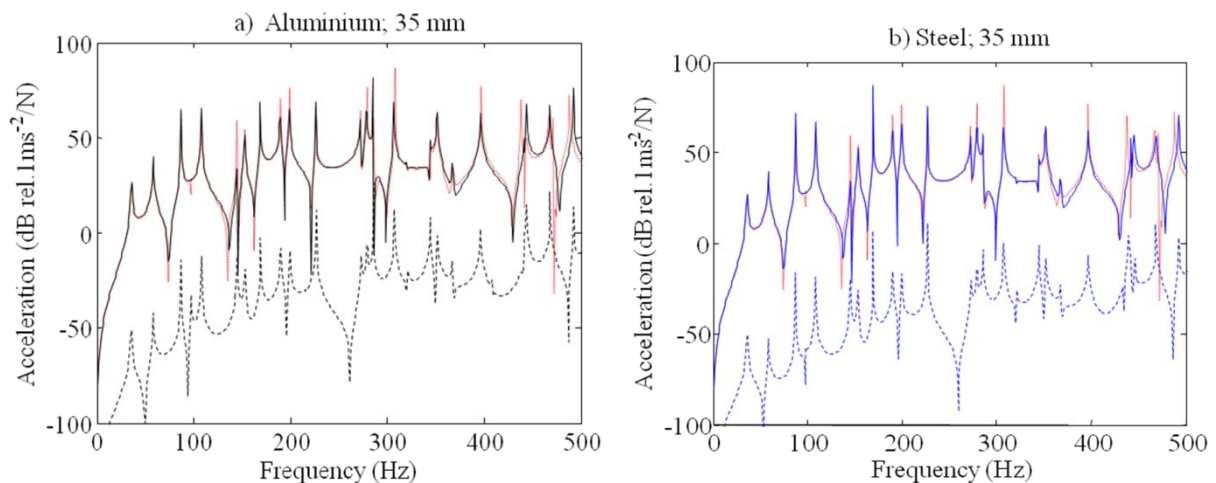


Figure 3: Force response measured either on the panel (solid lines) or on the front walls (dashed lines). The dotted lines show the forced response of an ideal test sample with clamped boundary conditions.

3.3 Coupled modes

In this subsection the acoustic coupling between the structure (panel-reinforced concrete walls) and the enclosed volume of the fluid (air) is presented. A comparison of the natural frequencies of the uncoupled plate+structure and the cavity system with those of the coupled plate-structure-cavity system is summarised in Table 1. The first column shows the natural frequencies of the sample panel with clamped boundary conditions. The geometry and properties of the sample panel are summarised in the Table 4. In the second column the natural frequencies due to the structure are listed. The third column shows the natural frequencies of the sample panel clamped to structure plus the frequencies due to structure itself. The fourth column shows the acoustic frequencies due to the cavity and the fifth column shows the coupled frequencies. It is seen that the modes controlled by the vibration of the plate+structure have frequencies slightly lower than those of the corresponding uncoupled plate modes. The natural frequencies of the modes controlled by the acoustic vibrations in the cavity are instead slightly higher than those of the corresponding uncoupled cavity modes.

A2 Panel with Clamped boundary conditions	Structures frequencies	Structure+Panel	Acoustic frequencies	Coupled modes
35.6539		35.6211		37.4634
58.3569		58.2878		57.5926
			151.3813	151.60583
152.7912		152.7531		152.58681
169.1599		169.0142		169.58475
			185.5101	185.19042
	445.60	448.0566		448.34946
			450.5839	451.60638
	446.98	456.897		456.91388
	579.92	580.8369		580.78628

Table 2: Coupled modes; panel, structure and acoustic frequencies

4 Final design

The transmission suite (acoustic cavity) is a reverberation chamber made of reinforced concrete and has a set of four aluminium front walls with different sample test window size:

- A2 size: the geometry parameters can be found in the Figure 7,
- A3 size: the geometry parameters can be found in the Figure 8,
- A4 size: the geometry parameters can be found in the Figure 9 and
- fully closed front wall: the geometry parameters can be found in the Figure 10.

Its volume is 0.8 m^3 and has no two parallel walls. The linear dimensions of the transmission suite are shown in Figure 4 (inner dimensions) and Figure 5 (outer dimensions). The reinforced wall thickness is 15 cm while the thickness of the aluminium front wall is 35 mm. The aluminium front walls are linked to the transmission suite by a steel frame (Figure 11) which is attached to the reinforced concrete acoustic cavity by a double row of 84 bolts screwed to the front frame (Figure 6). These two materials (aluminium front wall and front frame) are linked by a double row of bolts (84). A layer of rubber isolator is placed between

the aluminium front wall and the front frame in order to reduce transmission of vibration. The transmission suite is mounted in four air-springs in order to isolate it from any vibration coming from the floor.

The air-borne excitation is provided by two loudspeakers located in each of the rear corners of the acoustic cavity while the structural borne is provided by a point force produced by a shaker acting directly on the lightweight panel clamped to one of the aluminium front walls.

Material	Young's Modulus E (Nm ⁻²)	Density ρ (kgm ⁻³)	Absorption coefficient (α)
Steel	2.0 10 ¹¹	7.8 10 ³	
Aluminium	7.1 10 ¹⁰	2.7 10 ³	
Concrete (dense)	2.6 10 ¹⁰	2.3 10 ³	0.01

Table 3: Material properties for the Steel, Aluminium

Parameter	Value
Dimensions	$l_x \times l_y = 420 \times 594$ mm
Thickness	1 mm
Mass density	2700 kg/m ³
Young's modulus	$E=7.1_1010$ N/m ²

Table: Geometry and physical parameters for the clamped aluminium panel.

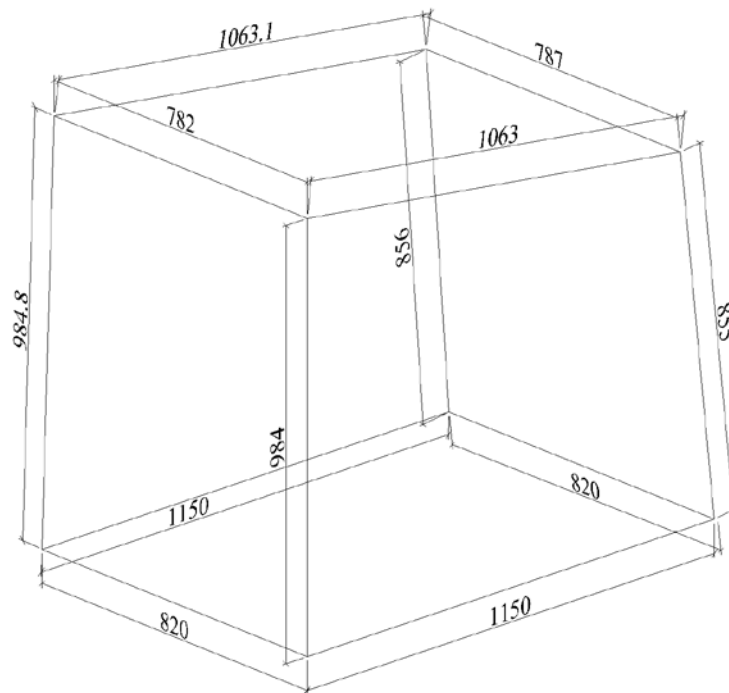


Figure 4: Inner dimensions.

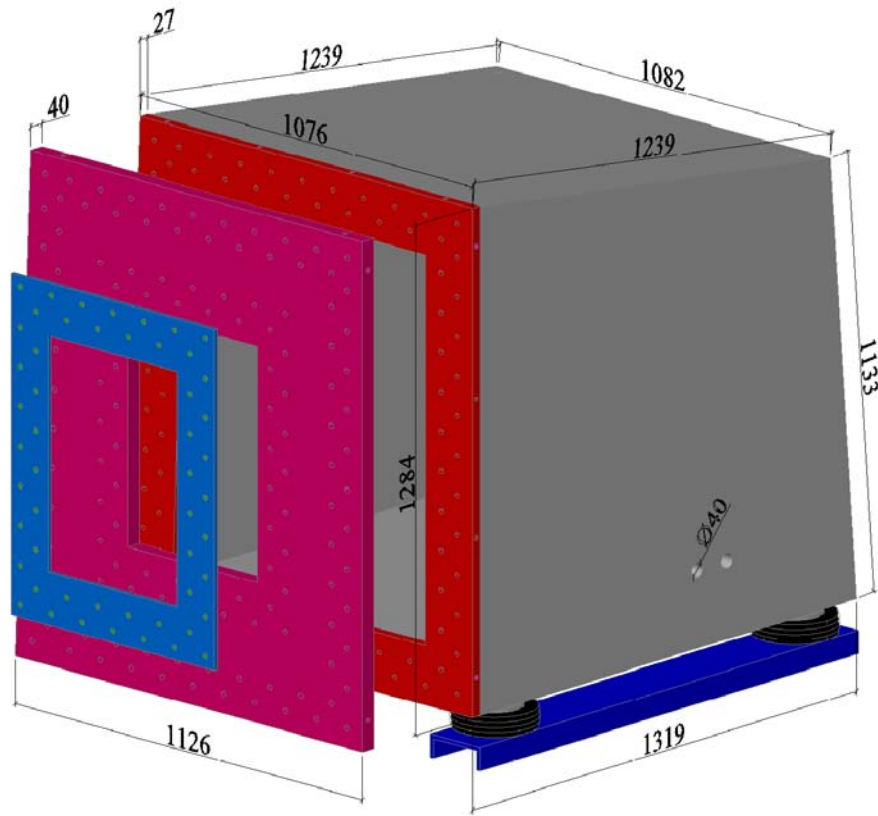


Figure 5: Final design; outer dimensions.

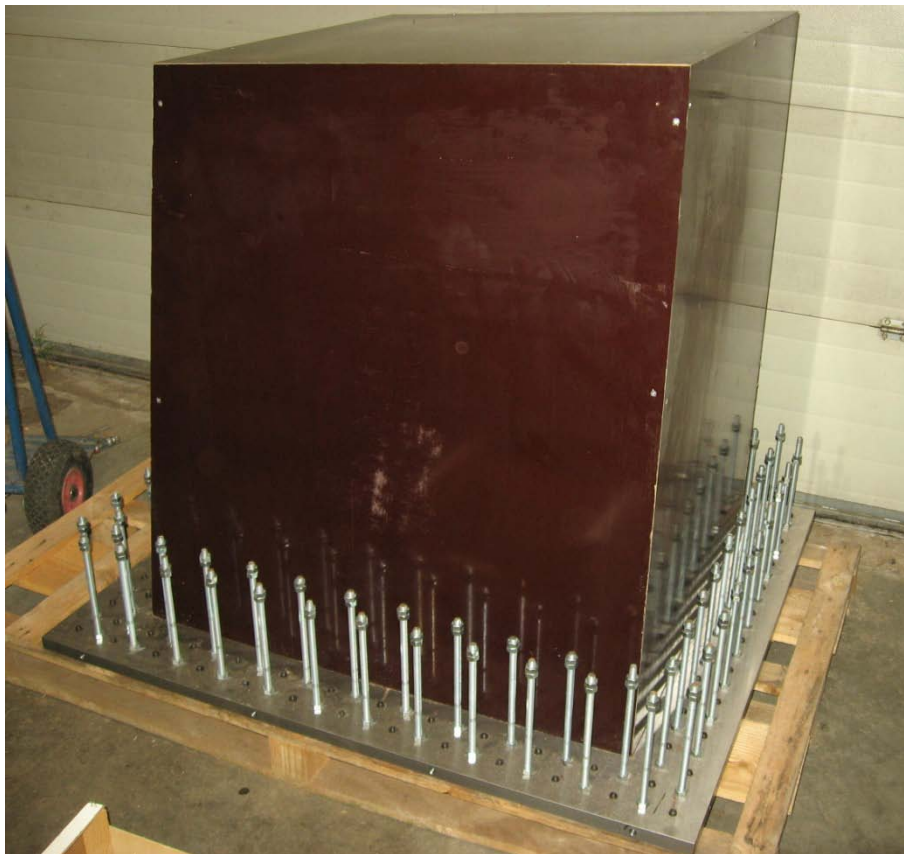


Figure 6: Front frame with bolts and inner formwork.

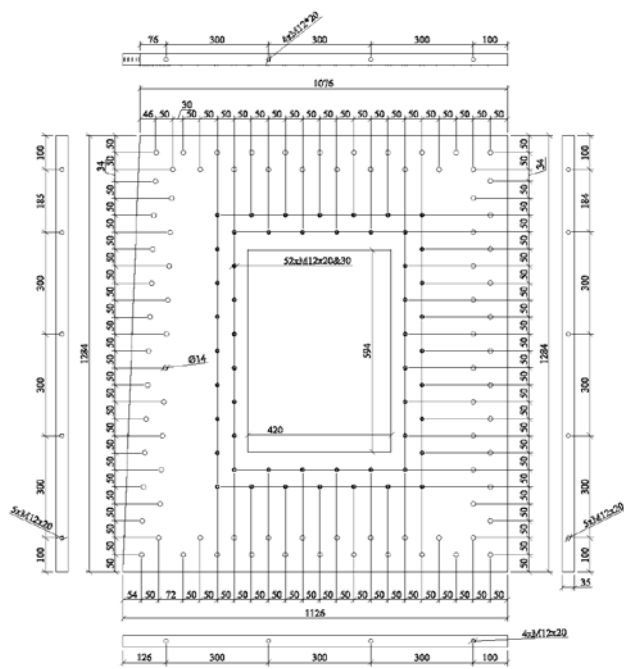


Figure 7: Front wall; A2 window size.

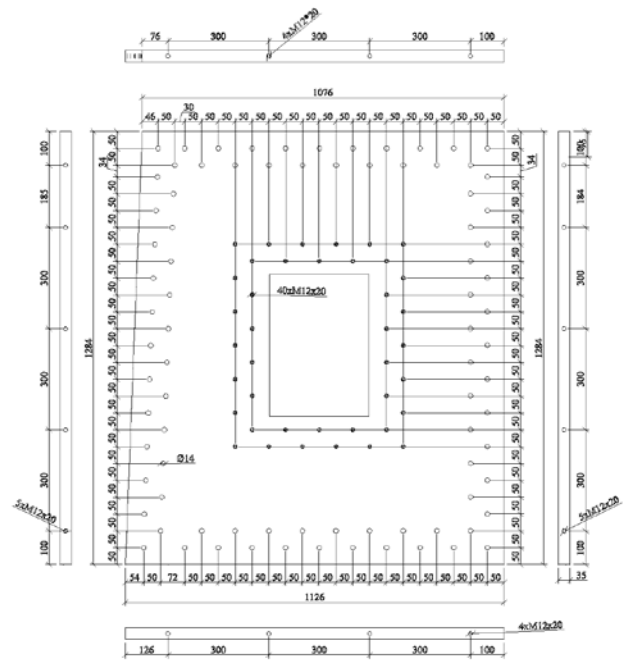


Figure 8: Front wall; A3 window size.

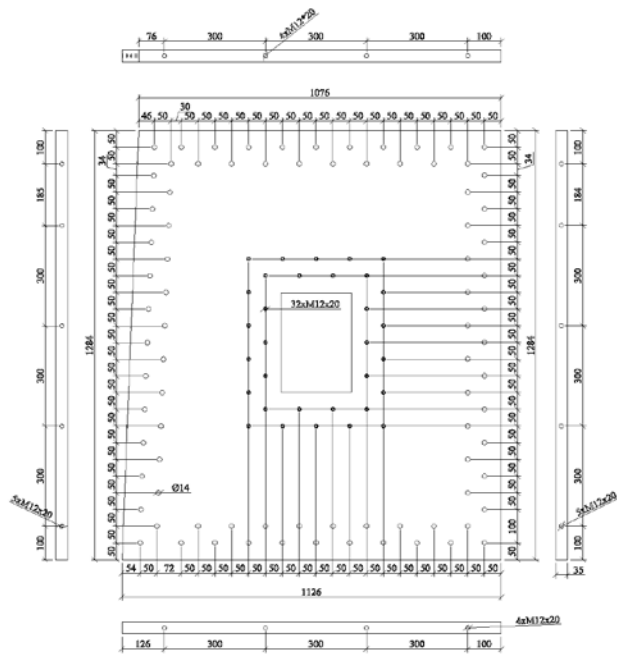


Figure 9: Front wall; A4 window size.

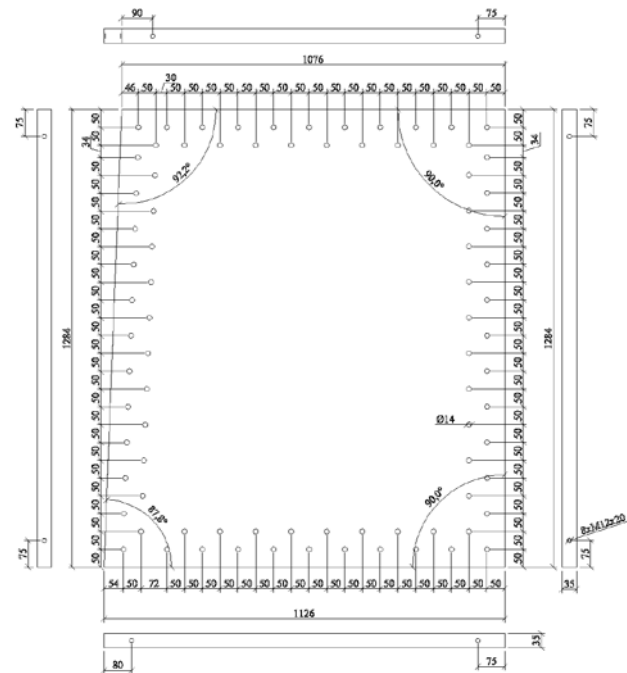


Figure 10: Fully closed front wall

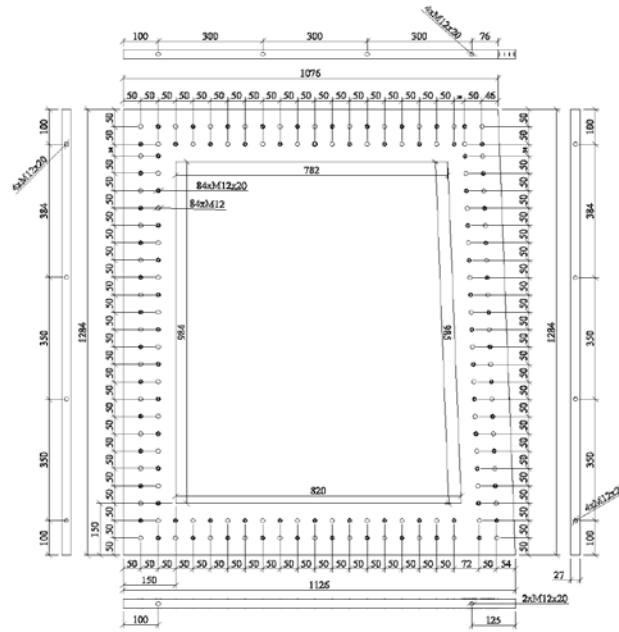


Figure 11: Front frame.

5 Conclusions and ongoing work

This paper describes the design of an acoustic cavity (transmission suite) in order to characterise the vibro-acoustic properties of lightweight panels. This acoustic room has the advantage of being relatively small; 1150x984x820 mm, which allows the identification of the studied behaviour for both structure- and air-borne excitation. The optimum geometric configuration has been found taking into account the acoustic eigenfrequencies' occurrences up to the Schroeder frequency and considering the surface averaged sound absorption coefficient (α). The shape proposed in this paper gives to the smoothest and most uniform distribution of the natural frequencies of the acoustic cavity.

The final design has no-parallel walls made of reinforced concrete. The setup has four set of front wall with different windows side in order to accommodate different sizes of lightweight materials. This setup allows the identification of both structure-borne and air-borne acoustic isolation parameters in lightweight panels of different sizes.

The setup is currently under construction and further works will aim to provide an experimental validation by comparing experimental results to a numerical model and simulation. Also, a convex shape has been chosen in order to be able to model it as a unique subsystem in the WBM.

Currently, a way to clamp the lightweight materials is been researched. This clamp mechanism should allow to clamp the lightweight materials in such a way that it does not damage them and a numerical model can be done in order to compare numerical model with experimental values.

Acknowledgements

The research was supported by the Research Training Network funded under the 6th Framework Programme of the European Commission under the project "Smart Structures – A Computer Aided Engineering Approach to Smart Structures" (<http://www.smart-structures.eu>, contract nr. MRTN-CT-2006-035559), from which the first author holds an Experienced Researcher Training Grant. Furthermore, the authors also kindly acknowledge the European Commission for their support of the Marie Curie EST Project SIMVIA2 (<http://www.simvia2.eu>, contract nr. MEST-CT-2005-020263), from which the second

author holds a Research Training grant. Also the Fund for Scientific Research - Flanders (F.W.O.), Belgium, is gratefully acknowledged for its research support.

References

- [1] S. MAKRIS, C. L. DYM, and J. SMITH, "Transmission loss optimization in acoustic sandwich panels," *Journal of the Acoustical Society of America*, vol. 79, 1933.
- [2] O. Elbeyli, P. Thamburaj, and J. Q. Sun, "Structural-acoustic studies of sandwich structures: A review," *Shock and Vibration Digest*, vol. 33, no. 5, pp. 372-384, 2001.
- [3] H. Denli and J. Q. Sun, "Structural-acoustic optimization of sandwich cylindrical shells for minimum interior sound transmission," *Journal of Sound and Vibration*, vol. 316, no. 1-5, pp. 32-49, 2008.
- [4] H. Denli, J. Q. Sun, and T. W. Chou, "Minimization of acoustic radiation from thick multilayered sandwich beams," *AIAA Journal*, vol. 43, no. 11, pp. 2337-2341, 2005.
- [5] H. Denli and J. Q. Sun, "Structural-acoustic optimization of sandwich structures with cellular cores for minimum sound radiation," *Journal of Sound and Vibration*, vol. 301, no. 1-2, pp. 93-105, 2007.
- [6] H. Denli and J. Q. Sun, "Structural-acoustic optimization of sandwich cylindrical shells for minimum interior sound transmission," *Journal of Sound and Vibration*, vol. 316, no. 1-5, pp. 32-49, 2008.
- [7] P. Wennhage, "Weight Optimization of Sandwich Panel with Acoustic Constraints, Experimental Verification," *Journal of Sandwich Structures and Materials*, pp. 353-365, Oct.2002.
- [8] A. C. Nilsson, "Reduction Index and Boundary-Conditions for A Wall Between 2 Rectangular Rooms .1. Theoretical Results," *Acustica*, vol. 26, no. 1, p. 1-&, 1972.
- [9] "Acoustics - Measurement of sound absorption in a reverberation room (ISO 354)," 2003.
- [10] "ASTM C423-08, Standard test method for sound absorption and sound absorption coefficients by the reverberation room method,".
- [11] "Acoustics - Determination of sound absorption coefficient and impedance in impedances tubes - Part 1: Method using standing wave ratio (ISO 10534-1) ," 2001.
- [12] "Acoustics - Determination of sound absorption coefficient and impedance in impedances tubes - Part 2: Transfer-function method (ISO 10534-1)," 2001.
- [13] R. H. Bolt, "Note on Normal Frequency Statistics for Rectangular Rooms," *The Journal of the Acoustical Society of America*, vol. 18, no. 1, pp. 130-133, July1946.
- [14] R. H. Bolt, "Frequency Distribution of Eigentones in a Three-Dimensional Continuum," *The Journal of the Acoustical Society of America*, vol. 10, no. 3, pp. 228-234, Jan.1939.
- [15] R. H. Bolt, "Normal Modes of Vibration in Room Acoustics: Angular Distribution Theory," *The Journal of the Acoustical Society of America*, vol. 11, no. 1, pp. 74-79, July1939.
- [16] R. H. Bolt, "Normal Frequency Spacing Statistics," *The Journal of the Acoustical Society of America*, vol. 19, no. 1, pp. 79-90, Jan.1947.

- [17] M. A. Blaszak, "Acoustic design of small rectangular rooms: Normal frequency statistics," *Applied Acoustics*, vol. 69, no. 12, pp. 1356-1360, Dec.2008.
- [18] M. R. Schroeder and K. H. Kuttruff, "On Frequency Response Curves in Rooms. Comparison of Experimental, Theoretical, and Monte Carlo Results for the Average Frequency Spacing between Maxima," *The Journal of the Acoustical Society of America*, vol. 34, no. 1, pp. 76-80, Jan.1962.
- [19] M. R. Schroeder, "The ``Schroeder frequency" revisited," *The Journal of the Acoustical Society of America*, vol. 99, no. 5, pp. 3240-3241, May1996.
- [20] W. C. Sabine, "The American Architect," 1900.
- [21] "American National Standard Institute (ANSI) S1.31: Broad-Band noise sources in reverberation rooms,".
- [22] "Acoustics -- Determination of sound power levels of noise sources using sound pressure -- Precision methods for reverberation rooms (ANSI/ASA S12.51-2002/ISO 3741:1999),".
- [23] B. Pluymers, B. Van Hal, D. Vandepitte, and W. Desmet, "Trefftz-based methods for time-harmonic acoustics," *Archives of Computational Methods in Engineering*, vol. 14, no. 4, pp. 343-381, 2007.